

This is the accepted manuscript made available via CHORUS. The article has been published as:

Shining Light on Transition-Metal Oxides: Unveiling the Hidden Fermi Liquid

Xiaoyu Deng, Aaron Sternbach, Kristjan Haule, D. N. Basov, and Gabriel Kotliar

Phys. Rev. Lett. **113**, 246404 — Published 8 December 2014

DOI: [10.1103/PhysRevLett.113.246404](https://doi.org/10.1103/PhysRevLett.113.246404)

Shining light on transition metal oxides: unveiling the hidden Fermi Liquid

Xiaoyu Deng,¹ Aaron Sternbach,² Kristjan Haule,¹ D. N. Basov,² and Gabriel Kotliar¹

¹*Department of Physics and Astronomy, Rutgers University, Piscataway, New Jersey 08854, USA*

²*Department of Physics, University of California-San Diego, La Jolla, California 92093, USA*

(Dated: November 11, 2014)

We use low energy optical spectroscopy and first principles LDA+DMFT calculations to test the hypothesis that the anomalous transport properties of strongly correlated metals originate in the strong temperature dependence of their underlying resilient quasiparticles. We express the resistivity in terms of an effective plasma frequency ω_p^* and an effective scattering rate $1/\tau_{tr}^*$. We show that in the archetypal correlated material V_2O_3 , ω_p^* increases with increasing temperature, while the plasma frequency from the partial sum rule exhibits the opposite trend. $1/\tau_{tr}^*$ has a more pronounced temperature dependence than the scattering rate obtained from the extended Drude analysis. The theoretical calculations of these quantities are in quantitative agreement with experiment. We conjecture that these are robust properties of all strongly correlated metals, and test it by carrying out a similar analysis on thin film $NdNiO_3$ on $LaAlO_3$ substrate.

PACS numbers: 71.27.+a, 72.10.-d, 78.20.-e

Understanding the transport properties in metallic states of strongly correlated materials is a long-standing challenge in condensed matter physics. Many correlated metals are not canonical Landau Fermi liquids (LFL) as their resistivities do not follow the T^2 law in a broad temperature range. Fermi liquid behavior emerges only below a very low temperature scale, T_{LFL} , which can be vanishingly small or hidden by the onset of some form of long range order. Above T_{LFL} , the resistivity usually rises smoothly and eventually exceeds the Mott-Ioffe-Regel limit, entering the so-called “bad metal” regime[1] with no clear sign of saturation [2, 3]. As stressed in Ref. 1 an interpretation of the transport properties in terms of quasiparticles (QPs) is problematic when the mean free path is comparable with the de Broglie wavelength of the carriers and describing the charge transport above T_{LFL} is an important challenge for the theory of strongly correlated materials.

It was shown in the context of the interacting electron phonon system, that the QP picture is actually valid in regimes that fall outside the LFL hypothesis[4]. There are peaks in the spectral functions which define renormalized QPs even though the QP scattering rate is comparable to the QP energy. The transport properties can be formulated in terms of a transport Boltzman kinetic equation for the QP distribution function, which has precisely the form proposed by Landau[5, 6]. Solving the transport equation, the dc conductivity can be expressed as

$$\sigma_{dc} = (\omega_p^*)^2 \tau_{tr}^* / 4\pi \quad (1)$$

in analogy with Drude formula. The effective transport scattering rate $1/\tau_{tr}^*$ characterizes the decay of QPs due to collisions involving Umklapp process, and ω_p^* is the low energy effective plasma frequency.

The temperature dependence of the transport coefficients beyond the scope of LFL and many salient features

seen in correlated oxides, such as their low coherence scale, non saturating resistivities and anomalous transfer of spectral weight, are described well in studies of doped Hubbard model within the framework of dynamical field mean theory (DMFT) (for early reviews of this topic see [7, 8]). A complete understanding of the transport anomalies has been reached recently[9–11]. As in the Prange-Kadanoff theory[4], the QPs are resilient, surviving in a broad region above T_{LFL} [10] and a quantum kinetic equation provides a quantitative description of the transport[11].

While in the electron-phonon coupled system treated in Ref. 4 the Fermi liquid parameters such as the QP velocities and therefore ω_p^* are temperature independent, they are strongly temperature dependent in the doped Mott insulator within DMFT due to changes in the Fermi surface at high temperatures [9, 10] and a strong temperature dependence of the effective mass at intermediate temperatures [10, 11]. This strong temperature dependence of ω_p^* hides the more conventional temperature dependence of $1/\tau_{tr}^*$ in the resistivity, which is quadratic in a broad region of temperatures and has saturating behavior at high temperatures [11]. Strong temperature dependence in the QP electronic structure with the resulting temperature dependence of ω_p^* and $1/\tau_{tr}^*$ thus provides a simple scenario to describe the anomalous transport of correlated metals.

In this Letter, we provide experimental and theoretical evidences that this picture holds beyond the DMFT treatment of simplified Hubbard Model, and is indeed relevant to real materials. We focus on V_2O_3 . This archetypal correlated material provided the first experimental corroboration of the validity of the DMFT picture of Mott transition[12] and is still a subject of intense experimental studies[13–17]. We extract the effective plasma frequency ω_p^* and effective scattering rate $1/\tau_{tr}^*$ from the optical conductivity as described below

and show that they display the predicted temperature dependence. We contrast their temperature dependence to that of the plasma frequency and scattering rate extracted from the standard extended Drude analysis.

In correlated systems the optical conductivity is usually parametrized with the so-called extended Drude analysis in terms of two frequency dependent quantities, the scattering rate $1/\tau(\omega)$ and the mass enhancement $m^*(\omega)/m_b$ [18],

$$\sigma(\omega) = \sigma_1(\omega) + i\sigma_2(\omega) = \frac{\omega_p^2}{4\pi} \frac{1}{-i\omega \frac{m^*(\omega)}{m_b} + 1/\tau(\omega)}. \quad (2)$$

The plasma frequency ω_p is obtained with the partial sum rule $\frac{\omega_p^2}{8} = \int_0^\Omega \sigma_1(\omega) d\omega$ and depends on the cutoff Ω chosen so as to exclude interband transitions. To test the theory, instead we focus on quantities that have a simple QP interpretation, namely $1/\tau_{tr}^*$ and $(\omega_p^*)^2$, from low frequency optical conductivity extracted as follows,

$$(\omega_p^*)^2 = 4\pi \frac{\sigma_1^2 + \sigma_2^2}{\sigma_2/\omega} \Big|_{\omega \rightarrow 0}, \quad 1/\tau_{tr}^* = \frac{\sigma_1}{\sigma_2/\omega} \Big|_{\omega \rightarrow 0}, \quad (3)$$

When a direct determination of the imaginary part of optical conductivity (as for example in ellipsometry measurements) is not available, they can be extracted from $\sigma_1(\omega)$ only, using

$$\frac{\sigma_2(\omega)}{\omega} \Big|_{\omega \rightarrow 0} = -\frac{1}{\pi} \int_{-\infty}^{\infty} \frac{1}{\omega'} \frac{\partial \sigma_1(\omega')}{\partial \omega'} d\omega'. \quad (4)$$

Comparing with extended Drude analysis, we have $(\omega_p^*)^2 = \frac{m_b}{m^*(0)} \omega_p^2$, $\frac{1}{\tau_{tr}^*} = \frac{m_b}{m^*(0)} \frac{1}{\tau(0)}$. Thus this analysis is related to extended Drude analysis, but free of partial sum rule. Similar low frequency analysis has been used in previous works [18–24], however the temperature dependence of ω_p^* and $\frac{1}{\tau_{tr}^*}$ was not the focus of those studies.

We apply the proposed analysis to V_2O_3 , a prototypical material exhibiting a metal insulator transition (MIT) [25, 26]. Pure V_2O_3 is a paramagnetic metal (PM) at ambient condition. It enters antiferromagnetic insulating state (AFI) below $T_N \simeq 150K$ with a concomitant structural transition, and the AFI can be quenched by Ti-doping or pressure. The PM can be turned into the paramagnetic insulator (PI) by slight Cr-doping, which induces a first order isostructural transition with a small change in c/a ratio, indicating a typical band-controlled MIT scenario [27]. This first order transition ends at a second order critical point at temperature around 400K [13, 26]. The PM phase exhibits significant signatures of correlations, for instance, a pronounced QP peak and a broad lower Hubbard band were revealed in photoemission spectroscopy measurements [28–30]. The PM phase is a Fermi liquid at low temperature when AFI state is suppressed [31].

Fig 1(a)(b) shows the measured optical conductivity $\sigma(\omega) = \sigma_1(\omega) + i\sigma_2(\omega)$ of pure V_2O_3 in PM phase [16].

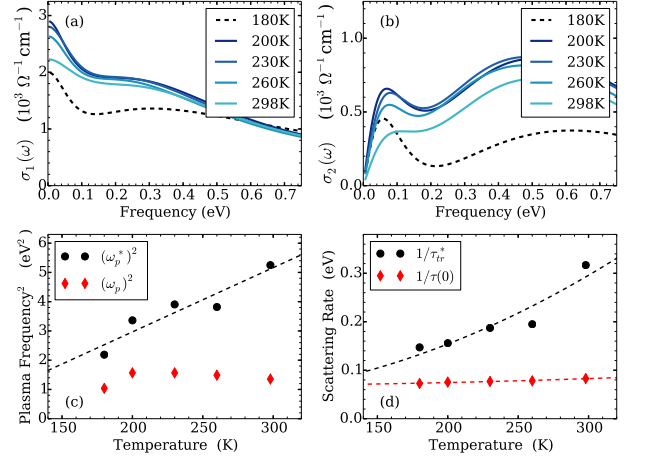


FIG. 1. Optical conductivity (a) $\sigma_1(\omega)$ and (b) $\sigma_2(\omega)$ of V_2O_3 at different temperature is taken from Ref. [16], where dashed lines indicate data at $T = 180K$ very close to MIT. (c) $(\omega_p^*)^2$ and (d) $1/\tau_{tr}^*$ of V_2O_3 are extracted according to Eqn. 3. ω_p^2 and $1/\tau(0)$ extracted from extended Drude analysis are shown for comparison. Dashed lines are guides for the eyes by fitting $(\omega_p^*)^2$ and $1/\tau_{tr}^*$ ($1/\tau(0)$) to linear ($a + bT$) and parabolic ($c + dT^2$) functions respectively.

Pronounced Drude peaks show up even when the resistivity is high (of the order of $1 m\Omega^{-1}cm^{-1}$) and does not follow T^2 -law [13, 32]. The Drude peak diminishes gradually upon increasing temperature, except at the lowest temperature where the transport is probably affected by the precursor of ordered phase. ω_p^* and $1/\tau_{tr}^*$ extracted according to Eqn. 3 are shown in Fig 1(c)(d). We find that $(\omega_p^*)^2$ increases with increasing temperature. This is in contrast with $(\omega_p)^2$ obtained by the partial sum rule with a cut off $\Omega = 140meV$, which slightly decreases [16] except at the lowest temperature where precursors to ordered phase such as magnetism and electronic heterogeneity tend to open a gap and reduce $(\omega_p)^2$. $1/\tau_{tr}^*$ increases with increasing temperature and has the same trend as the scattering rate extracted with extended Drude analysis at zero frequency $1/\tau(0)$, but with a much stronger temperature dependence. The experimental data is consistent with an $(\omega_p^*)^2$ which has a term linear and a $1/\tau_{tr}^*$ which is quadratic in temperature, revealing a Fermi liquid behavior that is hidden in $1/\tau_{tr}^*$. The analysis of the experimental data, thus corroborates the main qualitative predictions of the DMFT description of transport properties in simple model Hamiltonian [11].

We now argue that realistic LDA+DMFT [33, 34] calculations describe well the optical properties as well as the extracted quantities ω_p^* and $1/\tau_{tr}^*$, hence a local approximation, which ignores vertex corrections, is sufficiently accurate to capture the experimental trends. LDA+DMFT investigations on V_2O_3 by several groups have successfully described the properties of this material near the MIT [35–40]. The correlation in V_2O_3 is due to

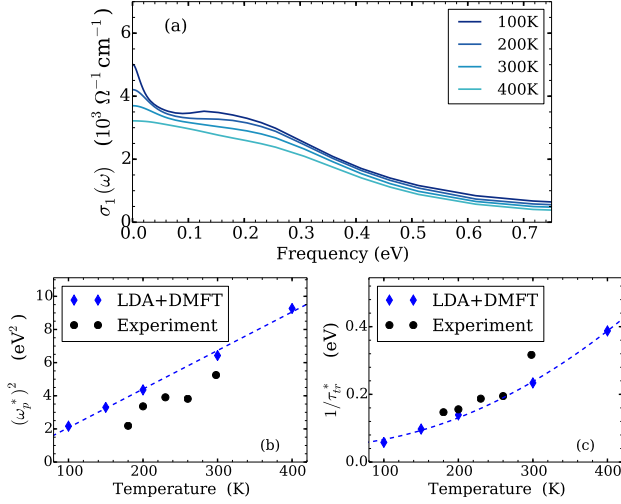


FIG. 2. (a) Optical conductivity of V_2O_3 calculated with LDA+DMFT. The effective plasma frequency (b) and effective scattering rate (c) are extracted using Eqn. 3, 4 and compared to those extracted from experimental data. Dashed lines are guides to the eyes by fitting $(\omega_p^*)^2$ and $1/\tau_{tr}^*$ to linear ($a + bT$) and parabolic ($c + dT^2$) functions respectively.

the partially filled narrow d -orbitals with a nominal occupancy $n_d = 2$. The two electrons mainly populate the e_g^π and a_{1g} states of vanadium due to surrounding oxygen octahedron with trigonal distortion. We perform the LDA+DMFT calculations and focus on the paramagnetic metallic phase only[41]. We treat e_g^π and a_{1g} orbitals dynamically with DMFT, and set the Coulomb interaction U and the Hund's coupling J to 6.0eV and 0.8eV respectively. These parameters place V_2O_3 on the metallic side but close to the MIT. Various properties of V_2O_3 from our calculations are in good agreement with experimental results. For example, the calculated total spectra is consistent with experiment photoemission spectroscopy measurements[28–30]. The occupancies of e_g^π and a_{1g} orbitals at $T = 200\text{K}$ are 1.60 and 0.50 respectively, in good agreement with X-ray absorption spectroscopy measurements[42].

We calculate the optical conductivity with the formalism presented in Ref. [43] in a broad temperature range as shown in Fig. 2(a). The main feature of the experimental optical conductivity, the Drude peak and the shoulder structure at about 0.1eV as well as their scale, are reasonably reproduced in our calculations. The Drude peak is gradually diminished and merges with the shoulder structure at around 400K, in agreement with experiments [44]. Therefore LDA+DMFT calculation provides a satisfactory description of the optical properties of V_2O_3 , except for the lowest temperature $T = 180\text{K}$ where effects such as short range order and heterogeneity in the proximity to the magnetic transition are not captured in our calculation. From the optical conductivity $(\omega_p^*)^2$ and $1/\tau_{tr}^*$ are extracted using Eqn. 3, 4. As shown in Fig 2(b)(c),

they agree reasonably well with those extracted from experimental data. In particular the same trends found with the experimental data, thus the main characteristics of the "hidden" Fermi liquid behavior, shows up more clearly in the broad temperature range studied in our calculations: $(\omega_p^*)^2$ appears linear and a $1/\tau_{tr}^*$ appears quadratic versus temperature. Therefore the proposed analysis of both the experimental data and the first principle calculations reveals significant temperature dependence of QPs in terms of $(\omega_p^*)^2$ and an extended quadratic temperature dependence of $1/\tau_{tr}^*$, but not of $1/\tau(0)$.

To further understand these observations, let us recall the QP interpretation of low frequency optical conductivity in the DMFT treatment of the doped single band Hubbard model. In this case, $\sigma(\omega)|_{\omega \rightarrow 0} = 2 \frac{m}{m^*} \Phi^{xx}(\bar{\mu}) \frac{1}{-i\omega + 2/\tau_{qp}^*}$, in which m^*/m and τ_{qp}^* are the effective mass enhancement and the life time of QPs, Φ is the transport function $\Phi^{xx}(\epsilon) = \sum_{\mathbf{k}} (\partial \epsilon_{\mathbf{k}} / \partial \mathbf{k}_x)^2 \delta(\epsilon - \epsilon_{\mathbf{k}})$ and $\bar{\mu}$ is the effective chemical potential of QPs[11]. Applying the analysis in Eqn. 3, $(\omega_p^*)^2 = 8\pi \frac{m}{m^*} \Phi^{xx}(\bar{\mu})$ and $1/\tau_{tr}^* = 2/\tau_{qp}^*$. In the infinite dimension limit where DMFT is exact, the inverse of effective mass enhancement m/m^* is numerically equal to the QP weight defined by $Z = (1 - \frac{\partial \text{Re}\Sigma(\omega)}{\partial \omega})^{-1}$, where $\Sigma(\omega)$ is the self energy. We note that in general the effective mass enhancement m^*/m enters the low frequency optical conductivity while the QP weight Z does not [5, 6]. We also note that the effective mass enhancement m^*/m does not enter the plasma frequency in the textbook example of interacting Fermi gas due to the presence of Galilean invariance and thus the cancellation of vertex correction and effective mass enhancement [5, 6]. However the vertex correction is weak in realistic materials (especially in three dimensional structure with a large coordination number), which are much closer to the infinite dimensional limit than the Galilean invariant idealization without important Umklapp process[45]. This justifies the good agreement between our results and experiments. The neglect of vertex correction in DMFT thus leaves QP weight in the plasma frequency. In situations where $\Phi(\bar{\mu})$ varies little with temperature, the observations above imply a strong temperature dependence of Z_{qp} and $1/\tau_{qp}^*$. We emphasize that although a strong dependence of scattering rate is generally expected in a Fermi liquid, the temperature dependence of QP weight is not, but it was observed in model studies[10, 11].

We then extract from our calculated self energies, the QP weight Z defined above, and the QP scattering rate defined as $2/\tau_{qp}^* = -2Z \text{Im}\Sigma(0)$, which now are orbital dependent. The QP weight and the QP scattering rate are shown in Fig. 3(a)(b). There is orbital differentiation between e_g^π and a_{1g} orbitals as pointed out in earlier studies [35, 37]. Generally Z increases with increasing temperature and $1/\tau_{qp}^*$ is approximately quadratic in temperature for both e_g^π and a_{1g} orbitals. a_{1g} orbital is

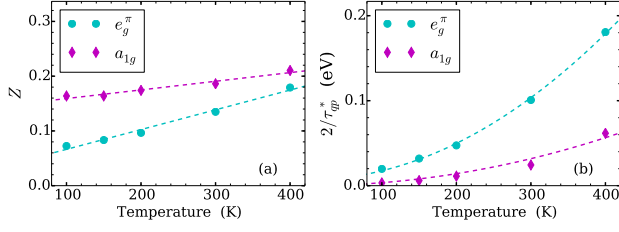


FIG. 3. The temperature dependence of (a) QP weight $Z = \frac{m}{m^*} = (1 - \frac{\partial \text{Re}\Sigma(\omega)}{\partial \omega})^{-1}$ and (b) effective scattering rate $2/\tau_{qp}^* = -2Z \text{Im}\Sigma(0)$ of V_2O_3 extracted from LDA+DMFT self energies for e_g^π and a_{1g} orbitals. Dashed lines are guides for the eyes by fitting Z and $2/\tau_{qp}^*$ to linear ($a + bT$) and parabolic ($c + dT^2$) functions respectively.

more coherent than e_g^π orbital: $Z_{a_{1g}}$ is less temperature dependent and the effective QP scattering rate is smaller. It likely crosses over to the LFL regime below $T \simeq 150\text{K}$ where $Z_{a_{1g}}$ starts to saturate. Note that e_g^π orbitals have a much larger spectral weight at the Fermi level than the a_{1g} orbital and thus dominate the transport. This pronounced temperature dependence is consistent with that of $(\omega_p^*)^2$ and $1/\tau_{tr}^*$ extracted from the optical conductivity. Therefore the properties of the underlying QPs, especially the temperature dependence of the QP weight and the QP scattering rate, are captured in our analysis on optical conductivities. We note that in addition the temperature dependence of underlying QPs manifest itself in the temperature dependence of the effective chemical potentials of QPs[41], which also contribute to the the temperature dependence of $(\omega_p^*)^2$.

We expect that this picture of anomalous transport in correlated materials is not limited to V_2O_3 and is in fact generally applicable to various strongly correlated metals. To check the validity of this general conjecture we apply the same analysis to experimental data of NdNiO_3 (NNO) film on LaAlO_3 (LAO) substrate. NNO is another typical correlated material exhibiting temperature-driven MIT[46]. While deposited as film on LAO substrate, the MIT can be quenched so that it remains metallic down to very low temperature [47]. High quality optical conductivities of NNO film are taken from Ref 48 as shown in Fig 4(a)(b). We note that the resistivity is not T^2 -like except possibly at the lowest temperature $T = 20\text{K}$ [47]. We perform the same analysis as above in V_2O_3 . $(\omega_p^*)^2$ and $1/\tau_{tr}^*$ are shown in Fig. 4(c)(d) in comparison with ω_p^2 and $1/\tau(0)$ obtained by extended Drude analysis with a cutoff of $\Omega = 125\text{meV}$. Again we have the same features as in V_2O_3 : $(\omega_p^*)^2$ increases almost linearly with increasing temperature and has the opposite trend with $(\omega_p)^2$, while $1/\tau_{tr}^*$ has a more pronounced quadratic behavior in a wide temperature range well above T_{LFL} .

In conclusion, in this Letter we point out and establish by analyzing both the experimental and the theoretical data that the anomalous transport properties observed in

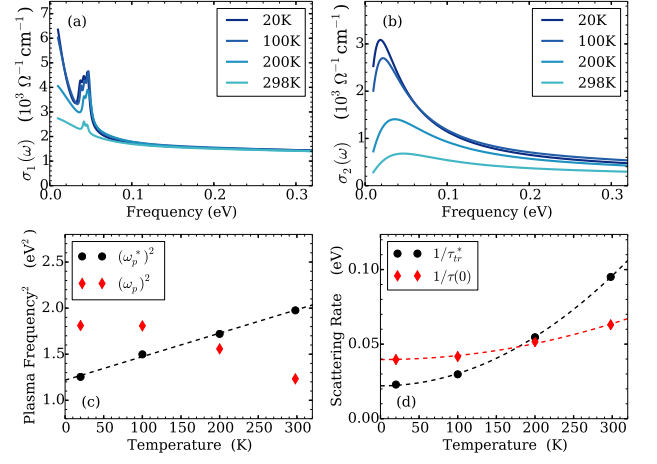


FIG. 4. Optical conductivity (a) $\sigma_1(\omega)$ and (b) $\sigma_2(\omega)$ of NNO film on LAO substrate at different temperature is taken from Ref. [48], from which (c) $(\omega_p^*)^2$ and (d) $1/\tau_{tr}^*$ are extracted according to Eqn. 3. ω_p^2 and $1/\tau(0)$ extracted from extended Drude analysis are shown for comparison. Dashed lines are guides for the eyes by fitting $(\omega_p^*)^2$ and $1/\tau_{tr}^*$ ($1/\tau(0)$) to linear ($a + bT$) and parabolic ($c + dT^2$) functions respectively.

many transition metal oxides arise from a temperature dependent $(\omega_p^*)^2$ and $1/\tau_{tr}^*$. The quadratic dependence of the QP scattering rate hidden from the resistivity is not confined to Mott Hubbard systems but occurs also in Hund's metal such as CaRuO_3 [41]. Further investigations should be carried out in other compounds, starting from systems where there are already preliminary indications such as nickelates, pnictides and cuprates [49–51], with a temperature dependent $m^*(0)/m_b$ seen in the extended Drude analysis. Finally high resolution studies using spectroscopies such as ARPES and STM in quasi-particle interference mode would be very useful to separate the various contributions to the temperature dependence of $(\omega_p^*)^2$ by probing directly the electronic structure.

We acknowledge very useful discussions with A. Georges and P. Armitage. This work was supported by NSF DMR-1308141 (X. D. and G.K.), NSF DMR 0746395 (K. H.) and DOE-BES (A. S. and D. B.). Computations were made possible using NSF EAGER DMR-1342921.

-
- [1] V. J. Emery and S. A. Kivelson, Phys. Rev. Lett. **74**, 3253 (1995).
- [2] N. Hussey, K. Takenaka, and H. Takagi, Phil. Mag. **84**, 2847 (2004).
- [3] O. Gunnarsson, M. Calandra, and J. E. Han, Rev. Mod. Phys. **75**, 1085 (2003).
- [4] R. E. Prange and L. P. Kadanoff, Phys. Rev. **134**, A566 (1964).
- [5] P. Nozieres and D. Pines, *Theory Of Quantum Liquids*.
- [6] P. Nozieres, *Theory Of Interacting Fermi Systems*.
- [7] T. Pruschke, M. Jarrell, and J. Freericks, Advances in Physics **44**, 187 (1995).
- [8] A. Georges, G. Kotliar, W. Krauth, and M. J. Rozenberg, Rev. Mod. Phys. **68**, 13 (1996).
- [9] G. Pálsson and G. Kotliar, Phys. Rev. Lett. **80**, 4775 (1998).
- [10] X. Deng, J. Mravlje, R. Žitko, M. Ferrero, G. Kotliar, and A. Georges, Phys. Rev. Lett. **110**, 086401 (2013).
- [11] W. Xu, K. Haule, and G. Kotliar, Phys. Rev. Lett. **111**, 036401 (2013).
- [12] M. J. Rozenberg, G. Kotliar, H. Kajueter, G. A. Thomas, D. H. Rapkine, J. M. Honig, and P. Metcalf, Phys. Rev. Lett. **75**, 105 (1995).
- [13] P. Limelette, A. Georges, D. Jerome, P. Wzietek, P. Metcalf, and J. M. Honig, Science **302**, 89 (2003).
- [14] S. Lupi, L. Baldassarre, B. Mansart, A. Perucchi, A. Barinov, P. Dudin, E. Papalazarou, F. Rodolakis, J.-P. Rueff, J.-P. Iti, S. Ravy, D. Nicoletti, P. Postorino, P. Hansmann, N. Parragh, A. Toschi, T. Saha-Dasgupta, O. K. Andersen, G. Sangiovanni, K. Held, and M. Marsi, Nature Communications **1**, 105 (2010).
- [15] F. Rodolakis, P. Hansmann, J.-P. Rueff, A. Toschi, M. W. Haverkort, G. Sangiovanni, A. Tanaka, T. Saha-Dasgupta, O. K. Andersen, K. Held, M. Sikora, I. Aliot, J.-P. Itié, F. Baudelet, P. Wzietek, P. Metcalf, and M. Marsi, Phys. Rev. Lett. **104**, 047401 (2010).
- [16] M. K. Stewart, D. Brownstead, S. Wang, K. G. West, J. G. Ramirez, M. M. Qazilbash, N. B. Perkins, I. K. Schuller, and D. N. Basov, Phys. Rev. B **85**, 205113 (2012).
- [17] Y. Ding, C.-C. Chen, Q. Zeng, H.-S. Kim, M. J. Han, M. Balasubramanian, R. Gordon, F. Li, L. Bai, D. Popov, S. M. Heald, T. Gog, H.-k. Mao, and M. van Veenendaal, Phys. Rev. Lett. **112**, 056401 (2014).
- [18] D. N. Basov, R. D. Averitt, D. van der Marel, M. Dressel, and K. Haule, Rev. Mod. Phys. **83**, 471 (2011).
- [19] W. Götze and P. Wölffe, Phys. Rev. B **6**, 1226 (1972).
- [20] J. W. Allen and J. C. Mikkelsen, Phys. Rev. B **15**, 2952 (1977).
- [21] S. Kamal, D. M. Kim, C. B. Eom, and J. S. Dodge, Phys. Rev. B **74**, 165115 (2006); S. Kamal, J. Dodge, D.-M. Kim, and C. B. Eom, in *Quantum Electronics and Laser Science Conference, 2005. QELS '05*, Vol. 1 (2005) pp. 443–445.
- [22] S. J. Youn, T. H. Rho, B. I. Min, and K. S. Kim, physica status solidi (b) **244**, 1354 (2007).
- [23] A. Millis, in *Strong interactions in low dimensions*, Physics and Chemistry of Materials with Low-Dimens, Vol. 25 (Springer Netherlands, 2004) pp. 195–235.
- [24] N. P. Armitage, (2009), arXiv:0908.1126.
- [25] D. B. McWhan, T. M. Rice, and J. P. Remeika, Phys. Rev. Lett. **23**, 1384 (1969).
- [26] D. B. McWhan, A. Menth, J. P. Remeika, W. F. Brinkman, and T. M. Rice, Phys. Rev. B **7**, 1920 (1973).
- [27] M. Imada, A. Fujimori, and Y. Tokura, Rev. Mod. Phys. **70**, 1039 (1998).
- [28] S.-K. Mo, J. D. Denlinger, H.-D. Kim, J.-H. Park, J. W. Allen, A. Sekiyama, A. Yamasaki, K. Kadono, S. Suga, Y. Saitoh, T. Muro, P. Metcalf, G. Keller, K. Held, V. Eyert, V. I. Anisimov, and D. Vollhardt, Phys. Rev. Lett. **90**, 186403 (2003).
- [29] F. Rodolakis, B. Mansart, E. Papalazarou, S. Gorovikov, P. Vilmercati, L. Petaccia, A. Goldoni, J. P. Rueff, S. Lupi, P. Metcalf, and M. Marsi, Phys. Rev. Lett. **102**, 066805 (2009).
- [30] H. Fujiwara, A. Sekiyama, S.-K. Mo, J. W. Allen, J. Yamaguchi, G. Funabashi, S. Imada, P. Metcalf, A. Higashiya, M. Yabashi, K. Tamasaku, T. Ishikawa, and S. Suga, Phys. Rev. B **84**, 075117 (2011).
- [31] D. B. McWhan, J. P. Remeika, J. P. Maita, H. Okinaka, K. Kosuge, and S. Kachi, Phys. Rev. B **7**, 326 (1973).
- [32] D. B. McWhan, J. P. Remeika, T. M. Rice, W. F. Brinkman, J. P. Maita, and A. Menth, Phys. Rev. Lett. **27**, 941 (1971).
- [33] G. Kotliar, S. Y. Savrasov, K. Haule, V. S. Oudovenko, O. Parcollet, and C. A. Marianetti, Rev. Mod. Phys. **78**, 865 (2006).
- [34] K. Held, Advances in Physics **56**, 829 (2007).
- [35] K. Held, G. Keller, V. Eyert, D. Vollhardt, and V. I. Anisimov, Phys. Rev. Lett. **86**, 5345 (2001).
- [36] M. S. Laad, L. Craco, and E. Müller-Hartmann, Phys. Rev. B **73**, 045109 (2006).
- [37] A. I. Poteryaev, J. M. Tomczak, S. Biermann, A. Georges, A. I. Lichtenstein, A. N. Rubtsov, T. Saha-Dasgupta, and O. K. Andersen, Phys. Rev. B **76**, 085127 (2007).
- [38] P. Hansmann, A. Toschi, G. Sangiovanni, T. Saha-Dasgupta, S. Lupi, M. Marsi, and K. Held, physica status solidi (b) **250**, 1251 (2013).
- [39] D. Grieger, C. Piefke, O. E. Peil, and F. Lechermann, Phys. Rev. B **86**, 155121 (2012).
- [40] J. M. Tomczak and S. Biermann, Journal of Physics: Condensed Matter **21**, 064209 (2009).
- [41] See Supplementary Materials at [url], which includes Refs.[[52–60]], for the details of the LDA+DMFT calculations, the temperature dependence of momentum-resolved spectra and QP bands of V_2O_3 and the hidden Fermi Liquid behavior in $CaRuO_3$.
- [42] J.-H. Park, L. H. Tjeng, A. Tanaka, J. W. Allen, C. T. Chen, P. Metcalf, J. M. Honig, F. M. F. de Groot, and G. A. Sawatzky, Phys. Rev. B **61**, 11506 (2000).
- [43] K. Haule, C.-H. Yee, and K. Kim, Phys. Rev. B **81**, 195107 (2010).
- [44] L. Baldassarre, A. Perucchi, D. Nicoletti, A. Toschi, G. Sangiovanni, K. Held, M. Capone, M. Ortolani, L. Malavasi, M. Marsi, P. Metcalf, P. Postorino, and S. Lupi, Phys. Rev. B **77**, 113107 (2008).
- [45] H. Maebashi and H. Fukuyama, Journal of the Physical Society of Japan **67**, 242 (1998).
- [46] J. B. Torrance, P. Lacorre, A. I. Nazzari, E. J. Ansaldo, and C. Niedermayer, Phys. Rev. B **45**, 8209 (1992).
- [47] J. Liu, M. Kareev, B. Gray, J. W. Kim, P. Ryan, B. Dabrowski, J. W. Freeland, and J. Chakhalian, Applied Physics Letters **96**, 233110 (2010).
- [48] M. K. Stewart, J. Liu, M. Kareev, J. Chakhalian, and

- D. N. Basov, Phys. Rev. Lett. **107**, 176401 (2011).
- [49] M. K. Stewart, C.-H. Yee, J. Liu, M. Kareev, R. K. Smith, B. C. Chapler, M. Varela, P. J. Ryan, K. Haule, J. Chakhalian, and D. N. Basov, Phys. Rev. B **83**, 075125 (2011).
 - [50] M. M. Qazilbash, J. J. Hamlin, R. E. Baumbach, L. Zhang, D. J. Singh, M. B. Maple, and D. N. Basov, Nat Phys **5**, 647 (2009).
 - [51] S. I. Mirzaei, D. Stricker, J. N. Hancock, C. Berthod, A. Georges, E. van Heumen, M. K. Chan, X. Zhao, Y. Li, M. Greven, N. Bari, and D. van der Marel, Proceedings of the National Academy of Sciences **110**, 5774 (2013).
 - [52] P. Blaha, K. Schwarz, G. K. H. Madsen, D. Kvasnicka, and J. Luitz, *WIEN2K, An Augmented Plane Wave + Local Orbitals Program for Calculating Crystal Properties* (Karlheinz Schwarz, Techn. Universität Wien, Austria, 2001).
 - [53] P. Werner, A. Comanac, L. de' Medici, M. Troyer, and A. J. Millis, Phys. Rev. Lett. **97**, 076405 (2006).
 - [54] K. Haule, Phys. Rev. B **75**, 155113 (2007).
 - [55] K. Inaba, A. Koga, S.-i. Suga, and N. Kawakami, Phys. Rev. B **72**, 085112 (2005).
 - [56] L. Klein, L. Antognazza, T. H. Geballe, M. R. Beasley, and A. Kapitulnik, Phys. Rev. B **60**, 1448 (1999).
 - [57] G. Cao, O. Korneta, S. Chikara, L. DeLong, and P. Schlottmann, Solid State Communications **148**, 305 (2008).
 - [58] M. Schneider, D. Geiger, S. Esser, U. S. Pracht, C. Stingl, Y. Tokiwa, V. Moshnyaga, I. Sheikin, J. Mravlje, M. Scheffler, and P. Gegenwart, Phys. Rev. Lett. **112**, 206403 (2014).
 - [59] A. Georges, L. d. Medici, and J. Mravlje, Annual Review of Condensed Matter Physics **4**, 137 (2013).
 - [60] Z. P. Yin, K. Haule, and G. Kotliar, Phys. Rev. B **86**, 195141 (2012).